International Journal of Physical Sciences and Engineering
Available online at www.sciencescholar.us
Vol. 4 No. 3, December 2020, pages: 27-37
e-ISSN : 2550-6943, p-ISSN : 2550-6951
https://doi.org/10.29332/ijpse.v4n3.611

Spectral Reflectance and Principal Component Analysis on the Distribution of Clove Vegetation Using Landsat 8

I Made Yuliara[a], Ni Nyoman Ratini[b], Windarjoto[c], Ni Komang Tri Suandayani[d]

Manuscript submitted: 9 October 2020, Manuscript revised: 18 November 2020, Accepted for publication: 27 December 2020

Corresponding Author [a]

Keywords

clove distribution;
Landsat 8;
normalized difference vegetation index (NDVI);
principal component analysis (PCA);
spectral reflectance;

Abstract

This paper discusses the distribution of clove vegetation in Buleleng Regency, Bali using a vegetation index extracted from Landsat 8 imagery based on spectral reflectance and Principal Component Analysis (PCA). Data analysis used the Normalized Difference Vegetation Index (NDVI) transformation and PCA band transformation. Adjustment of the position of clove vegetation in the image is determined by the measurement results of the clove coordinate sample in the field. The results showed that the accuracy of the area of clove vegetation distribution as measured as a percentage comparison to the area data of the Forestry and Plantation Service, Buleleng Regency, Bali in 2014, was 97.066% for the spectral reflectance-based vegetation index ($NDVI_{ref}$) and 97.072% for those based on PCA ($NDVI_{pca}$). The distribution class category with the dominant area identified into heavy class ($NDVI_{ref}$) of 7841.25 ha and moderate class ($NDVI_{pca}$) of 7591.77 ha. There is a difference in the two determinant coefficient values (R^2), which is 0.2407% and at 5% significance, the variants of the B4 and B5 spectral reflectance image variable data variants, as well as the C1 and C2 component image variables simultaneously, can affect the NDVI vegetation index.

Contents

[a] Physics Departement, Faculty of Mathematics and Science, Udayana University, Denpasar, Bali, Indonesia
[b] Physics Departement, Faculty of Mathematics and Science, Udayana University, Denpasar, Bali, Indonesia
[c] Physics Departement, Faculty of Mathematics and Science, Udayana University, Denpasar, Bali, Indonesia
[d] Physics Departement, Faculty of Mathematics and Science, Udayana University, Denpasar, Bali, Indonesia

1 Introduction

The response of the spectral reflectance of an object is a function of the wavelength which is constructed from the reflection or emission of electromagnetic energy at different wavelengths. In remote sensing satellites, the spectral reflectance of objects on the earth's surface is represented by the pixel values in the satellite image data. Yuliara & Kasmawan (2017), conducted a study on the spectral reflectance of clove vegetation using Landsat 8 multispectral (multiband) satellite imagery in 2014 and found that the highest average spectral reflectance value was 66.08% (band 5) and the average smallest average 3, 49% (band 2).

Multiband satellite sensors record electromagnetic radiation from various parts of the spectrum that has the potential to have a high correlation in 1 data set, especially in the closest band (Rees, 2013). Apart from the advantages of the data dimension and the high correlation of the pixel values in the nearest band, difficulties and weaknesses in the further analysis will occur when multitemporal data are involved (Abd El-Kawy et al., 2011). The correlation between bands also causes the information contained in each band to not complement each other and the data tends to be redundant so that the information in the image is reduced, the resulting interpretation and estimation is less accurate. To eliminate information and reduce redundant data dimensions, a data transformation is needed, namely Principal Component Analysis (PCA) (Estornell et al., 2013; Destefanis et al., 2000; Lasaponara, 2006). PCA is a spectral data transformation that can make multiband images uncorrelated and independent and the main components produced can be used as input data for further image analysis such as building vegetation indices and object classification processes (Dharani & Sreenivasulu, 2019; Ozdogan, 2010; Rees, 2013).

Multiband satellite imagery is widely used in various studies related to global-scale vegetation which can effectively monitor plant biomass, map land dryness, Leaf Area Index (LAI), deforestation, chlorophyll concentration to estimate productivity (Adams & Gillespie, 2006; Dou et al., 2018; Houborg et al., 2015; Malatesta et al., 2013; Sule & Wood, 2020). Vegetation inventory, level of the greenness of the vegetation canopy, leaf area, and structure can be analyzed through the vegetation index (Lemenkova, 2015). Vegetation indexes can be extracted from multiband satellite data such as Landsat 8 where the vegetation index is a development of information technology that plays an important role in the engineering of information processes regarding both environmental and production assessments in modern agricultural systems (Xu & Guo, 2014; Houborg et al., 2015; Yuliara et al., 2018; Zaitunah et al., 2018). The calculation of the vegetation index involves the two-way spectral radiance reflectance factor at near-infrared (NIR, λ=0.845 - 0.885 μm) and red (λ=0.630 - 0.680 μm) (Rees, 2013).

The use of Landsat 8 multiband satellite imagery as an instrument in monitoring and analyzing the distribution and spectral reflectance characteristics of objects is quite a lot (Jagalingam et al., 2015; Roy et al., 2016). The advantages of the specification of Landsat 8 satellite imagery include good spatial and temporal resolution as well as spectral resolution with a large number of bands. With this specification, data analysis using PCA allows changes in estimation accuracy in identifying vegetation distribution (Dharani & Sreenivasulu, 2019). This study aims to determine (1) the distribution of clove vegetation using Landsat 8 in Buleleng Regency, Bali in 2014 based on spectral reflectance and PCA, and (2) the effect of spectral reflection and PCA transformation on the vegetation index in identifying clove distribution.

2 Materials and Methods

In this study, the material used is Landsat 8 imagery, recorded on May 5, 2014 path = 117, line = 66 and May 30, 2014 path = 116, line = 66 with the study area located at coordinates 8°03'40'' – 8°23'00'' South Latitude and 114°25'55'' – 15°27 '28' 'East Longitude as shown in Figure 1.

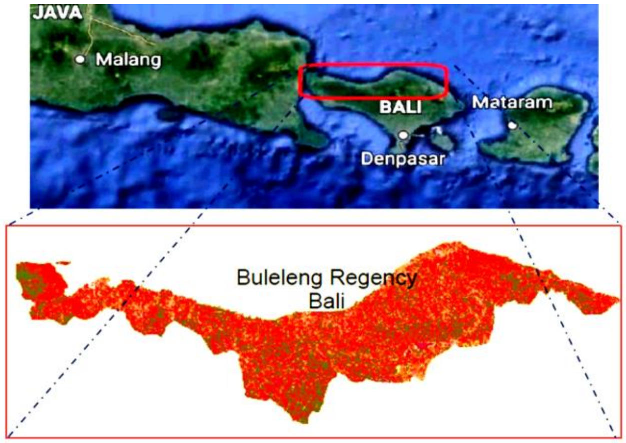

Figure 1. Location of the study area

Spectral reflectance calibration is performed on the Top Of Atmosphere (TOA) with correction of the sun's angle using the USGS EROS Center formula, namely (USGS, 2019):

$$\rho_\lambda = \frac{\rho'_\lambda}{\cos\theta_{SZ}} = \frac{\rho'_\lambda}{\sin\theta_{SE}} = \frac{M_\rho Q_{cal} + A_\rho}{\sin\theta_{SE}} \tag{1}$$

Where:

- ρ'_λ : is the value of spectral reflectance without correction for the angle of the sun
- M_ρ : is band-specific multiplicative rescaling factor, where x is the Band in EFLECTANCE_MULT_BAND_x
- A_ρ : is band-specific additive rescaling factor of metadata, where x is Band in EFLECTANCE_ADD_BAND_x
- Q_{cal} : is quantized and calibrated standard product pixel values (DN)
- θ_{SE} : is local sun elevation angle. The scene center the sun elevation angle in degrees (SUN_ELEVATION).
- θ_{SZ} : is local solar zenith angle; $\theta_{SZ} = 90° - \theta_{SE}$

The measurement of the coordinates of the clove vegetation sample in the field is carried out by selecting location points where the clove vegetation is quite homogeneous using the Global Positioning System (GPS) Smartphone. The geometric correction refers to the 9 Ground Control Points (GCPs) which is carried out using the nearest neighbor method. To clarify the visual interpretation and highlight the vegetation aspects, stretching was carried out using the Linear with Saturation method (Lillesand et al., 2015). The component image was obtained by performing a PCA transformation on each image band from the spectral reflectance calibration using the modules provided in the Idrisi TerrSet 18.21 software. The distribution of clove vegetation was analyzed using the NDVI vegetation index which was built based on a spectral reflectance image ($NDVI_{ref}$) and the main component image resulting from PCA transformation ($NDVI_{pca}$) using equation (Rees, 2013) :

$$NDVI = \frac{\rho_{NIR} - \rho_{Red}}{\rho_{NIR} + \rho_{Red}} \tag{2}$$

Where :

ρ_{NIR} is the reflectance in the Near Infrared band

ρ_{Red} is the reflectance in the Red band

Identification of the clove vegetation index is obtained by adjusting the measurement results of the clove vegetation coordinates in the field with the pixel coordinates in the image. The distribution of clove vegetation was estimated using the Cross Tabulation (CrossTab) method and the results were analyzed statistically descriptively with average area data from the Forestry and Plantation Service of Buleleng regency in 2014 as a reference. More, processing and analyzing image data is presented in Figure 2.

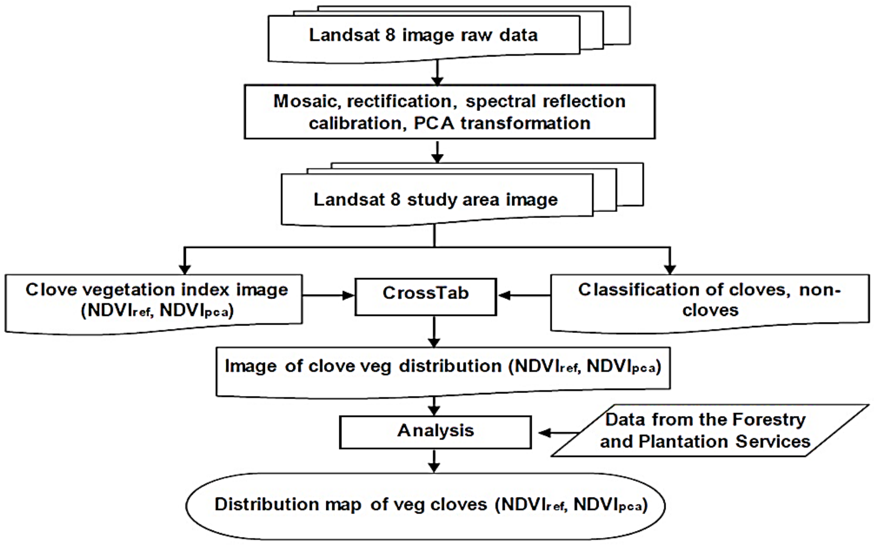

Figure 2. Research flow chart

3 Results and Discussions

3.1 Results

Image of study area B5 mosaicking results and spectral reflectance calibration results for the 2014 recording, May 5 with θ_{SE} = 53.22614231 and May 30 with θ_{SE} = 49.29799717 are presented in Figure 3a. The image of the study area of the main component C1 transformed by PCA using the PCA module on TerrSet 18.21 with Pallete quant is presented in Figure 3b.

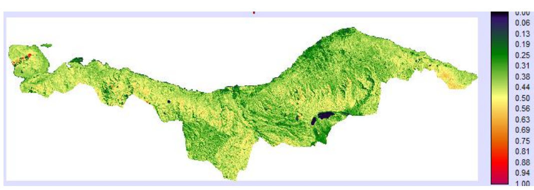
Figure 3a. Image of B5 spectral reflectance

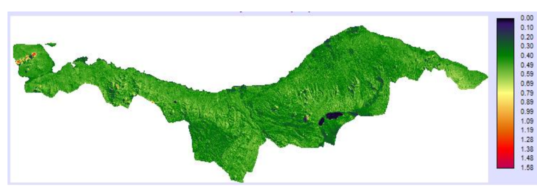
Figure 3b. Image of the main component of C1

Characteristic curves of average pixel values for the 6 bands (B2, B3, B4, B5, B6, B7) at 10 observation points (OP) are presented in Figure 4a and for the 6 components (C1, C2, C3, C4, C5, C6) are presented in Figure 4b. The classification process to distinguish clove and non-clove objects using the hard classification type and the calculation of the accuracy-test with a confusion matrix resulted in an overall accuracy of 89.16%. The vegetation index distribution image based on spectral reflectance ($NDVI_{ref}$) and based on PCA ($NDVI_{pca}$) calculated using equation (2) is presented in Figure 5a and Figure 5b.

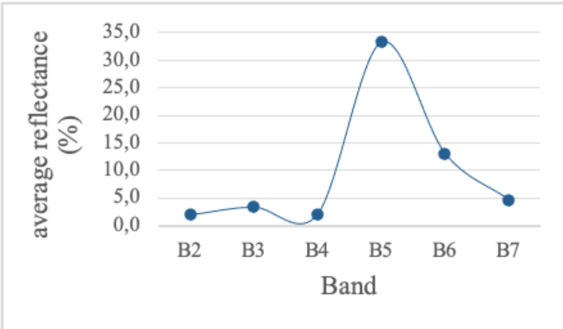

Figure 4a. Characteristics of the average pixel value of the image spectral reflectance

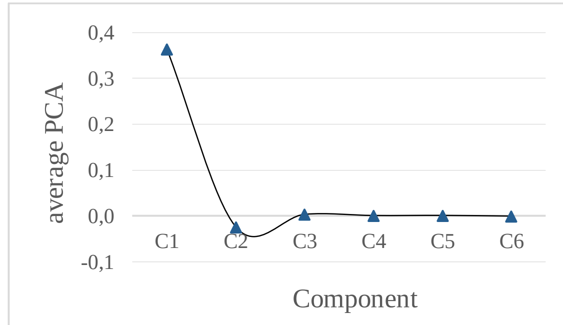

Figure 4b. Characteristics of the average pixel value of the PCA component image

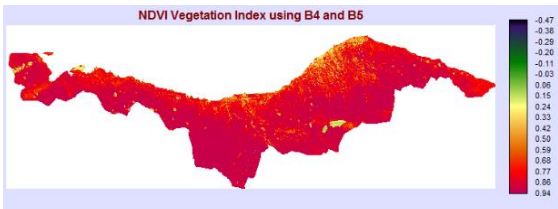

Figure 5a. $NDVI_{ref}$ distribution image

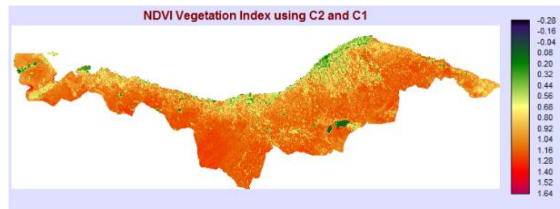

Figure 5b. $NDVI_{pca}$ distribution image

The results of coordinate measurements in the field are used as indicators of the position of clove vegetation on the coordinates of Landsat 8 images. The pixel values in the image of the study area for the $NDVI_{ref}$ and $NDVI_{pca}$ vegetation index model images at 10 OP are presented in Table 1. Comparison graphs of vegetation index values based on $NDVI_{ref}$ spectral reflectance and those based on PCA, $NDVI_{pca}$ on the survey coordinates are presented in Figure 6.

Table 1
Measurement results for the vegetation index value at 10 OP

OP	Geographical Coordinate (m)		Vegetation Index		$\Delta = NDVI_{pca} - NDVI_{ref}$
	Latitude (X)	Longitude (Y)	$NDVI_{ref}$	$NDVI_{pca}$	
1	295080	9092700	0.87424	1.07377	0.19953
2	295140	9092876	0.85774	1.03331	0.17557
3	294840	9093986	0.87300	1.08860	0.21560
4	295050	9093055	0.89188	1.12982	0.23793
5	284370	9083666	0.90065	1.23339	0.33274
6	295260	9092336	0.85820	1.02749	0.16929
7	307110	9098875	0.88453	1.14266	0.25813
8	306240	9099837	0.89576	1.22027	0.32451
9	306420	9099475	0.89139	1.21225	0.32086
10	307590	9097255	0.89990	1.26069	0.36080

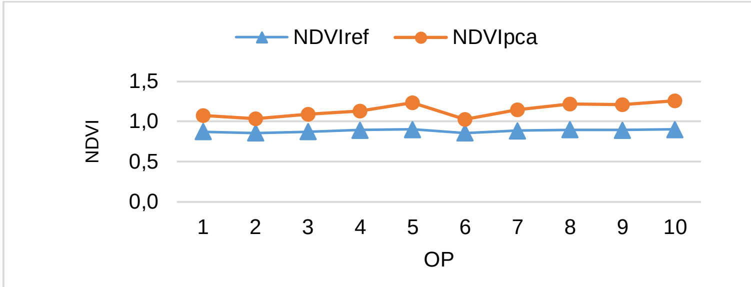

Figure 6. NDVI curve based on spectral reflectance and PCA at 10 OP

Correlation and the effect of spectral reflectance (B4 and B5) on the $NDVI_{ref}$ vegetation index and main components (C1 and C2) on the $NDVI_{pca}$ vegetation index, analyzed by multiple regression. $NDVI_{ref}$ as the dependent variable and as the independent variable B4 and B5. Likewise for $NDVI_{pca}$ as the dependent variable, C1, and C2 as the independent variable. A summary of the multiple regression results processed using the Statistics, Regression Analysis module contained in TerrSet 18.21 is presented in Table 2.

Table 2
Summary of multiple regression results

Variable		R	R^2	Regression equation
Dependent	Independent			
$NDVI_{ref}$	B4; B5	0.976062	0.952697	$NDVI_{ref} = 0.012941 - 2.035107*B4 + 2.147082*B5$
$NDVI_{pca}$	C2; C1	0.974828	0.950290	$NDVI_{pca} = 0.015602 - 3.116130*C2 + 2.165234*C1$

The results of vegetation index distribution image processing where the pixels are indicated as classified clove vegetation from $NDVI_{ref}$ is presented in Figure 7a, while for $NDVI_{pca}$ is presented in Figure 7b. The results of the calculation of the accuracy-test for the classification of clove and non-clove objects using a configuration matrix resulted in an overall accuracy of 91.64% for $NDVI_{ref}$ and $NDVI_{pca}$ of 92.04%.

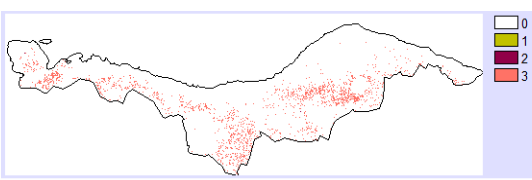

Figure 7a. $NDVI_{ref}$ index distribution image

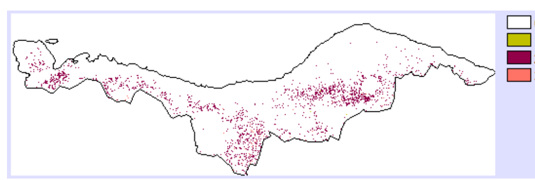

Figure 7b. $NDVI_{pca}$ index distribution image

The results of the area estimate and classification of clove vegetation distribution classes obtained through statistical analysis (CrossTab) are presented in Table 3. According to data from Dinas Kehutanan dan Perkebunan Pemkab Buleleng (DKP) (2014), the area of clove plantations in 2014 in Buleleng Regency, Bali is 7622.32 ha. Comparison of the estimated area of clove vegetation using $NDVI_{ref}$ and $NDVI_{pca}$ with clove vegetation area data from DKP of Buleleng Regency in 2014 is presented in Table 4.

Table 3
Estimated area of clove vegetation distribution based on $NDVI_{ref}$ and $NDVI_{pca}$

No.	Vegetation Index Models	Estimated Area (ha)	Area of Clove Vegetation Distribution Class (ha)		
			Rarely	Moderate	Heavy
1	$NDVI_{ref}$	7852.68	0.45	10.98	7841.25
2	$NDVI_{pca}$	7852.23	24.93	7591.77	235.53
Difference		0.45	24.48	7580.79	7605.72

Table 4
Comparison of $NDVI_{ref}$ and $NDVI_{pca}$ areas with DKP data in Buleleng Regency]

No.	Vegetation Index Models	Area (ha)	The average area of DKP data (ha)	Percentage (%)
1	$NDVI_{ref}$	7852.68	7622.32	97.066
2	$NDVI_{pca}$	7852.23	7622.32	97.072

The spatial information in the form of a map of the distribution of clove vegetation is the result of the application of the NDVI vegetation index theory based on spectral reflectance and based on the PCA transformation method on Landsat 8 satellite imagery. Map of the distribution of clove vegetation in Buleleng Regency, Bali based on spectral reflectance is presented in Figure 8a, while the PCA based is presented in Figure 8b.

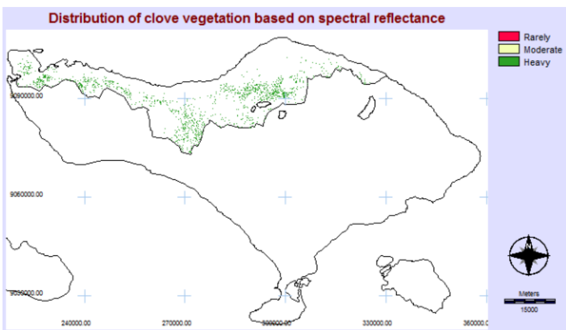

Figure 8a. $NDVI_{ref}$ based clove vegetation distribution map

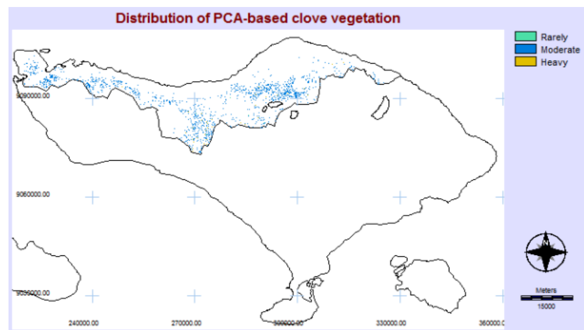

Figure 8b. $NDVI_{pca}$ based clove vegetation distribution map

3.2 Discussions

In terms of quality and quantity, image processing gives good results, such as the results of geometric corrections and resample, the total value of Root Mean Square (RMS) is 12.73. This result is less than ½ the pixel size, which is 30 m, very good in providing certainty of the position of objects in the image and making the image already have a reference (georegistration) at the UTM coordinates of the 50N zone (Liu & Xia, 2010). Contrast stretching using the Linear with Saturation method results in better visualization compared to single-band images and visually different objects appear more clearly visible (Lillesand et al., 2015; Liu & Xia, 2010).

Visually, the image of the spectral reflectance calibration is different from the image resulting from the PCA transformation as shown in Figure 3a and Figure 3b. In the component image, it is clear that after the application of the PCA transformation there is a reduction in data dimensions, data variability is reduced, eliminating redundant data in the spectral reflectance image. The pixel value of the image in both the spectral reflectance image and the main component image of PCA represents the object reflectance value (Dharani & Sreenivasulu, 2019; Shahabi et al., 2012). The size of the pixel value is described as the characteristic curve of the average pixel value for each band of the spectral reflectance image and the characteristic curve of the PCA component image as shown in Figures 4a and 4b.

From Figure 4a, it can be seen that the largest pixel value is in the B5 image (NIR, λ = 0.845 - 0.885 μm) and the smallest is in the B4 image (red, λ = 0.630 - 0.680 μm), while from Figure 4b the largest pixel value is in Figure 4a. image C1 and the smallest in image C2. The large pixel value in the image band and the main component image of PCA shows that the percentage of electromagnetic wave energy reflection from vegetation objects is greater than the percentage of energy absorbed. From Figure 3a and Figure 3b, it can be analogized that the spectral reflectance value (pixel value) in images B5 = C1 and B4 = C2. The largest and smallest spectral reflectance values of this vegetation are unique characteristics and are often used to analyze the greenness of vegetation, such as creating vegetation index images.

The two NDVI vegetation index images, both based on spectral reflectance in Figure 5a and PCA-based in Figure 5b, are visually different and provide different variability in pixel values (Shahabi et al., 2012; Sukmono & Ardiansyah, 2017). The difference in index values as shown in the data in Table 1 occurs at each OP location which describes the condition of the relevant vegetation. In general, the higher the vegetation index value indicates the condition of the clove vegetation, the healthier or more fertile and dense the condition of the clove vegetation is and actively carries out the photosynthesis process (Xue & Su, 2017; Yuliara & Kasmawan, 2017).

Figure 6 shows the difference in the trend of the vegetation index value curve on the NDVI vegetation index which is made from or based on the spectral reflectance value and the value based on the PCA component value. The roles of B4 and B5 in forming $NDVI_{ref}$ and the roles of C1 and C2 in forming $NDVI_{pca}$ are largely determined by the variability of the data or variants that represent the objects contained in the spectral reflectance images B4, B5 and C1, C2 component images. The biggest difference in NDVI value was at OP 10, which was 0.36080 and the smallest difference was at OP 6, which was 0.16929. In general, the differences in each OP arise because of changes in data variability on the 2 vegetation indices, namely $NDVI_{ref}$ and $NDVI_{pca}$.

The results of multiple regression analysis as presented in Table 2, get a coefficient of determination of $R^2 = 0.952697$ for the $NDVI_{ref}$ vegetation index which indicates that 95.2697% of variables B4 and B5 can explain the $NDVI_{ref}$ vegetation index while 4.7303% are explained or caused by variables other than B4 and B5. The correlation of variables B4 and B5 with $NDVI_{ref}$ is very strong as represented by the correlation coefficient value of R = 0.976062 which also means that 97.6062% of variables B4 and B5 affect the $NDVI_{ref}$ vegetation index. Likewise, for the $NDVI_{pca}$ vegetation index, it was obtained $R^2 = 0.950290$ which indicated that 95.0290% of the C1 and C2 variables could explain the $NDVI_{pca}$ vegetation index, and 4.971% was explained by variables other than C1 and C2. The correlation of variables C1 and C2 with $NDVI_{pca}$ is very strong as represented by the correlation coefficient value of R = 0.974828 which also means that 97.4828% of variables C1 and C2 affect the $NDVI_{pca}$ vegetation index.

From Table 3, the area estimate obtained from the $NDVI_{ref}$ vegetation index model is 7852.68 ha, which is greater than the area estimate from the $NDVI_{pca}$ vegetation index model, which is 7852.23 ha. A very small difference in area estimate resulted, namely 0.45 ha (5 pixels) inseparable from the difference in the vegetation index value indicated as clove vegetation as a result of spectral reflection and main component image (Shahabi et al., 2012; Bhandari et al., 2012; Becker & Choudhury, 1988). When compared with the average area from DKP data of Buleleng Regency, which is 7622.32 ha, the difference in the area estimation results given by $NDVI_{ref}$ is 228.36 ha and for $NDVI_{pca}$ the difference is 229.91 ha. When displayed in the form of spatial information or maps, the distribution of clove vegetation based on spectral reflectance as shown in Figure 8a is different from those based on PCA which are presented in Figure 8b.

4 Conclusion

Based on the results and data analysis obtained, the conclusions of this study are:

1) There is a difference in estimating the area of distribution of clove vegetation using $NDVI_{ref}$ and using $NDVI_{pca}$, which is 0.45 ha. The categories of distribution classes that were identified as dominant were heavy class ($NDVI_{ref}$) with an area of 7841.25 ha and medium-class ($NDVI_{pca}$) with an area of 7591.77 ha.
2) In identifying the distribution of clove vegetation, at the 5% significance and 95% confidence level, the simultaneous effect of spectral reflectance images (B4 and B5) on the $NDVI_{ref}$ vegetation index was 97.6062% and the effect of PCA component images (C1 and C2) simultaneously on $NDVI_{pca}$ amounted to 97.4828%.

Acknowledgments
The authors would like to thank Udayana University for funding this research through the Leading Research Scheme from the Study Program, the year 2020.

References

Abd El-Kawy, O. R., Rød, J. K., Ismail, H. A., & Suliman, A. S. (2011). Land use and land cover change detection in the western Nile delta of Egypt using remote sensing data. *Applied geography*, *31*(2), 483-494. https://doi.org/10.1016/j.apgeog.2010.10.012

Adams, J. B., & Gillespie, A. R. (2006). *Remote sensing of landscapes with spectral images: A physical modeling approach*. Cambridge University Press.

Becker, F., & Choudhury, B. J. (1988). Relative sensitivity of normalized difference vegetation index (NDVI) and microwave polarization difference index (MPDI) for vegetation and desertification monitoring. *Remote Sensing of Environment*, *24*(2), 297-311. https://doi.org/10.1016/0034-4257(88)90031-4

Bhandari, A. K., Kumar, A., & Singh, G. K. (2012). Feature extraction using Normalized Difference Vegetation Index (NDVI): A case study of Jabalpur city. *Procedia technology*, *6*, 612-621. https://doi.org/10.1016/j.protcy.2012.10.074

Destefanis, G., Barge, M. T., Brugiapaglia, A., & Tassone, S. (2000). The use of principal component analysis (PCA) to characterize beef. *Meat science*, *56*(3), 255-259. https://doi.org/10.1016/S0309-1740(00)00050-4

Dharani, M., & Sreenivasulu, G. (2019). Land use and land cover change detection by using principal component analysis and morphological operations in remote sensing applications. *International Journal of Computers and Applications*, 1-10.

Dinas Kehutanan dan Perkebunan Pemkab Buleleng. 2014. Laporan Triwulan Luas Areal dan Produksi Komoditas Perkebunan Kabupaten Buleleng Tahun 2014. Buleleng, Bali. [Indonesian]

Dou, Z., Cui, L., Li, J., Zhu, Y., Gao, C., Pan, X., ... & Li, W. (2018). Hyperspectral estimation of the chlorophyll content in short-term and long-term restorations of mangrove in Quanzhou Bay Estuary, China. *Sustainability*, *10*(4), 1127.

Estornell, J., Martí-Gavliá, JM, Sebastiá, MT, & Mengual, J. (2013). Principal component analysis applied to remote sensing. *Modeling in Science Education and Learning* , *6* , 83-89.

Houborg, R., Fisher, J. B., & Skidmore, A. K. (2015). Advances in remote sensing of vegetation function and traits. https://doi.org/10.1016/j.jag.2015.06.001

Jagalingam, P., Akshaya, B. J., & Hegde, A. V. (2015). Bathymetry mapping using Landsat 8 satellite imagery. *Procedia Engineering*, *116*, 560-566. https://doi.org/10.1016/j.proeng.2015.08.326

Lasaponara, R. (2006). On the use of principal component analysis (PCA) for evaluating interannual vegetation anomalies from SPOT/VEGETATION NDVI temporal series. *Ecological modelling*, *194*(4), 429-434. https://doi.org/10.1016/j.ecolmodel.2005.10.035

Lemenkova, P. (2015). Analysis of Landsat NDVI time series for detecting degradation of vegetation. In *Geoecology and Sustainable Use of Mineral Resources. From Science to Practice. Proceedings of 3rd International Conference of Young Scientists. Belgorod State University (BelSU), Ed. AN Petin, PV Goleusov, EI Makaseeva* (pp. 11-13).

Lillesand, T., Kiefer, R. W., & Chipman, J. (2015). *Remote sensing and image interpretation*. John Wiley & Sons.

Liu, D., & Xia, F. (2010). Assessing object-based classification: advantages and limitations. *Remote Sensing Letters*, *1*(4), 187-194.

Malatesta, L., Attorre, F., Altobelli, A., Adeeb, A., De Sanctis, M., Taleb, N. M., ... & Vitale, M. (2013). Vegetation mapping from high-resolution satellite images in the heterogeneous arid environments of Socotra Island (Yemen). *Journal of Applied Remote Sensing*, *7*(1), 073527.

Ozdogan, M. (2010). The spatial distribution of crop types from MODIS data: Temporal unmixing using Independent Component Analysis. *Remote Sensing of Environment*, *114*(6), 1190-1204. https://doi.org/10.1016/j.rse.2010.01.006

Rees, W. G. (2013). *Physical principles of remote sensing*. Cambridge university press.

Roy, D. P., Kovalskyy, V., Zhang, H. K., Vermote, E. F., Yan, L., Kumar, S. S., & Egorov, A. (2016). Characterization of Landsat-7 to Landsat-8 reflective wavelength and normalized difference vegetation index continuity. *Remote sensing of Environment*, *185*, 57-70. https://doi.org/10.1016/j.rse.2015.12.024

Shahabi, H., Ahmad, B. B., Mokhtari, M. H., & Zadeh, M. A. (2012). Detection of urban irregular development and green space destruction using normalized difference vegetation index (NDVI), principal component analysis (PCA) and post classification methods: A case study of Saqqez city. *International Journal of Physical Sciences*, *7*(17), 2587-2595.

Sukmono, A., & Ardiansyah. (2017). Identification of rice field using Multi-Temporal NDVI and PCA method on Landsat 8 (Case Study: Demak, Central Java). In *IOP Conference Series: Earth and Environmental Science* (Vol. 54, No. 1, p. 012001). IOP Publishing.

Sule, S. D., & Wood, A. (2020). Application of principal component analysis to remote sensing data for deforestation monitoring. In *Remote Sensing for Agriculture, Ecosystems, and Hydrology XXII* (Vol. 11528, p. 1152806). International Society for Optics and Photonics.

USGS. 2019. Using the USGS Landsat Level-1 Data Product.

Xu, D., & Guo, X. (2014). Compare NDVI extracted from Landsat 8 imagery with that from Landsat 7 imagery. *American Journal of Remote Sensing*, *2*(2), 10-14.

Xue, J., & Su, B. (2017). Significant remote sensing vegetation indices: a review of developments and applications. J Sens 2017: 1353691.

Yuliara, I. M., & Kasmawan, A. (2017). The Reflectance Spectral Characteristic of Cloves Vegetation Using Landsat 8 in Buleleng, Bali. *Journal of Food Security and Agriculture*, *1*(1), 15-18.

Yuliara, I. M., Sutapa, G. N., & Kasmawan, G. A. (2018). Development and optimization of the ratio vegetation index on the visible and infrared spectrum. *International journal of physical sciences and engineering*, *2*(2), 101-110.

Zaitunah, A., Samsuri, A. A., & Safitri, R. A. (2018, March). Normalized difference vegetation index (ndvi) analysis for land cover types using landsat 8 oli in besitang watershed, Indonesia. In *IOP Conference Series: Earth and Environmental Science* (Vol. 126, No. 1, pp. 1-9).

Biography of Authors

I Made Yuliara lives at Jalan Kedondong No. 8 Denpasar, Bali, Ph. 08123644116. He was born on July 18, 1964. He finished the Bachelor of Physics Program at Airlangga University in Surabaya, 1994. He completed the Master of Remote Sensing Program at the Institute of Technology on 10 November in Surabaya, 2000.
Email: imdyuliara@unud.ac.id

Ni Nyoman Ratini lives at Jalan Lingkar Timur Unud Perumahan Panorama Jimbaran Blok B No. 21 Bukit Jimbaran, Ph. 08123895890. She was born in April 1, 1967. She finished Bachelor of Physics Program at Airlangga University in Surabaya, 1992. She completed Master of Physics Science Program at Institute of Technology Bandung in Bandung, 2001.
Email: n_ratini@yahoo.com

Windarjoto is a Physics lecturer with a concentration in the field of Instrument Physics. Born in Surabaya on January 08, 1957, he worked in the Department of Physics at the Faculty of Mathematics and Natural Sciences, Udayana University, Bali since 1989.
Email: windaryoto@unud.ac.id

Ni Komang Tri Suandayani, S.Si, M.Si. Jembrana, 17 December 1970. Lecturer in Physics FMIPA Udayana University from 1999 to the present. Lecturer in Geophysics.
Email: tri_suandayani@unud.ac.id